

J. M. Lloris · B. León · C. Pérez Vicente · J. L. Tirado
M. Womes · J. Olivier Fourcade · J. C. Jumas

Composition and electrochemical properties of $\text{LiCu}_x\text{Mn}_{2-x}\text{O}_4$ and $\text{LiCu}_{0.5-y}\text{Al}_y\text{Mn}_{1.5}\text{O}_4$

Received: 1 April 2003 / Accepted: 2 June 2003 / Published online: 20 April 2004
© Springer-Verlag 2004

Abstract In order to gain a better understanding of the parameters affecting the capacity and performance of spinel electrode materials, the chemical composition and cation distribution of three members of the $\text{LiCu}_x\text{Mn}_{2-x}\text{O}_4$ and $\text{LiCu}_{0.5-y}\text{Al}_y\text{Mn}_{1.5}\text{O}_4$ series have been studied by chemical analysis, X-ray diffraction and X-ray absorption spectroscopy. The synthesis used stoichiometric and lithium-excess precursors. The results evidence that lithium is always incorporated in lower contents than expected from the nominal stoichiometry, owing to the occurrence of significant amounts of copper in the tetrahedral sites of the structure. Manganese displays an oxidation state below 4+ in all these solids, while the lithium-excess synthesis leads to a slightly higher average oxidation state. The electrochemical results evidence the lack of improvement in capacity by using lithium-excess synthesis, while a significant increase in capacity is obtained by aluminium doping, reaching values of 100 mAh/g.

Keywords Lithium batteries · Lithium–manganese spinel oxide · Positive electrode · Copper substitution

Introduction

Cathode materials for Li-ion cells are generally based on LiCoO_2 , LiNiO_2 and spinel LiMn_2O_4 [1, 2]. LiMn_2O_4 is currently a very promising cathode material owing to its economical and environmental advantages as compared with LiCoO_2 . However LiMn_2O_4 has been shown to exhibit poor cycling behaviour. To overcome this

problem the partial substitution of Mn by other transition metals has been proposed to give $\text{Li}M_x\text{Mn}_{2-x}\text{O}_4$, where M is Mg, Cr, Co, Ni, Cu, Fe or Zn or a mixture of them [3, 4, 5, 6, 7]. Some of these partial substitutions improved the capacity and potential, resulting in cathode materials with “high” potential (those offering a voltage between 4.5 and 5.1 V versus Li^+/Li).

Concerning more specifically the spinel oxide systems based on Li, Cu and Mn, previous results reported in the literature showed that nonstoichiometric compounds are obtained with copper in tetrahedral positions, accompanied by the presence of impurities of MnO_x , having a negative influence on the lithium insertion/extraction process. Two plateaus characterize the electrochemical charge curves of this system at 4.1 and 4.9 V, the total capacity being about 70 mAh/g [8]. In opposition to the low value of the capacity delivered by this system, a stable life cycle was reported for $\text{LiCu}_{0.5}\text{Mn}_{1.5}\text{O}_4$ [5]. Taking into account the nominal composition of these samples one should expect an oxidation state of the Mn ion close to 4.0, but electrochemical studies show that the plateau at 4.1 V is very important; therefore, the average oxidation state of Mn is significantly below 4.0.

To gain better understanding of the parameters affecting the capacity and performance of these electrode materials and to modify the synthesis conditions in order to increase the oxidation state of Mn, a series of $\text{LiCu}_x\text{Mn}_{2-x}\text{O}_4$ spinels was prepared as reference materials. Then doped materials with nominal composition $\text{LiCu}_xM_y\text{Mn}_{2-x-y}\text{O}_4$ were obtained and their electrochemical performances in lithium cells was compared to select the best dopant: Al. A combined X-ray absorption and diffraction study together with detailed chemical analysis gave new information on the oxidation states and cation distribution of these spinel oxide materials.

Experimental

A series of samples with nominal $\text{LiCu}_x\text{Mn}_{2-x}\text{O}_4$ (with $x=0.45, 0.5$ and 0.55) stoichiometry was prepared by a

J. M. Lloris · B. León · C. Pérez Vicente · J. L. Tirado (✉)
Laboratorio de Química Inorgánica,
Universidad de Córdoba, Edificio C3, planta 1,
Campus de Rabanales, 14071 Córdoba, Spain
E-mail: iq1ticoj@uco.es

M. Womes · J. Olivier Fourcade · J. C. Jumas
Laboratoire des Agrégats Moléculaires et Matériaux Inorganiques,
UMR 5072 CNRS, Université Montpellier II,
Place Eugène Bataillon, 34095 Montpellier, France

sol-gel procedure. Stoichiometric mixtures of Cu, Mn and Li acetates were added to a water-ethanol (75:25 v/v) solution. The slurries were slowly heated up to 200 °C to dryness. The products were then heated at different temperatures (700, 750 and 800 °C) for 24 h, and then reannealed for 24 h at 750 °C. It was previously shown that the use of lithium excess during the synthesis of lithium nickel oxide could improve the electrochemical performance [9]. Thus, $\text{LiCu}_{0.5}\text{Mn}_{1.5}\text{O}_4$ was also synthesized using an excess of lithium acetate (5% lithium excess). Finally, the different doped samples were also prepared by a sol-gel method with the addition to the solution of $\text{Al}(\text{OH})_3$, H_3BO_3 , $\text{Co}(\text{CH}_3\text{COO})_2$, $\text{Fe}(\text{COO})_2$ and $\text{C}_{12}\text{H}_{28}\text{O}_4\text{Ti}$ to yield B-, Al-, Co-, Fe- and Ti-doped compounds with $\text{LiCu}_{0.5-y}\text{M}_y\text{Mn}_{1.5}\text{O}_4$ stoichiometry.

X-ray diffraction patterns were recorded using a Siemens D5000 diffractometer, using Cu $K\alpha$ radiation. Mn L_{23} X-ray absorption measurements were carried out using the synchrotron radiation of the SACO storage ring of LURE, Orsay, France. The spectra were recorded by measuring the photoelectron current (photoelectron yield) with a channeltron detector. The beamline was equipped with a grazing monochromator. The energy step width employed for all spectra was 0.1 eV.

Some of the $\text{LiCu}_{0.5-y}\text{M}_y\text{Mn}_{1.5}\text{O}_4$ samples were analysed after being dissolving in HCl by flame atomic absorption spectroscopy (PerkinElmer 3100) for Li, Cu and Mn content. Furthermore the metal content (gram equivalent- M content, where M is Cu plus Mn) in the same samples was determined by a titration method with ethylenediaminetetraacetate. About 30 mg of sample was dissolved in the minimum amount of HCl, then ammonium solution was added to basic pH and the solution was titrated with a 0.05 M solution of ethylenediaminetetraacetate.

Electrochemical studies were carried out using a MacPile multichannel instrument under potentiostatic conditions, in steps of 50 mV per 0.1 h. Electrodes were cast on an aluminium foil from a slurry of 86% of the active material, 8% of a mixture of carbon black and graphite in a 1:1 weight proportion and 6% of poly(vinylidene fluoride) using 1-methyl-2-pyrrolidone as a solvent. The Swagelok-type cells were assembled inside an Ar-filled glove box (O_2 , H_2O less than 1 ppm), using Li metal as the counter electrode and a solution of 1 M LiPF_6 in ethylene carbonate/diethyl carbonate (in 1:1 weight proportion) as the electrolyte.

Results and discussion

Structural study

The X-ray diffraction patterns of samples with nominal composition $\text{LiCu}_x\text{Mn}_{2-x}\text{O}_4$ and $\text{LiCu}_{0.49}\text{Al}_{0.01}\text{Mn}_{1.5}\text{O}_4$, heated and reannealed at 750 °C, are shown in Fig. 1. The $\text{LiCu}_{0.55}\text{Mn}_{1.45}\text{O}_4$ sample (Fig. 1, pattern b) showed impurities of manganese and lithium, copper mixed

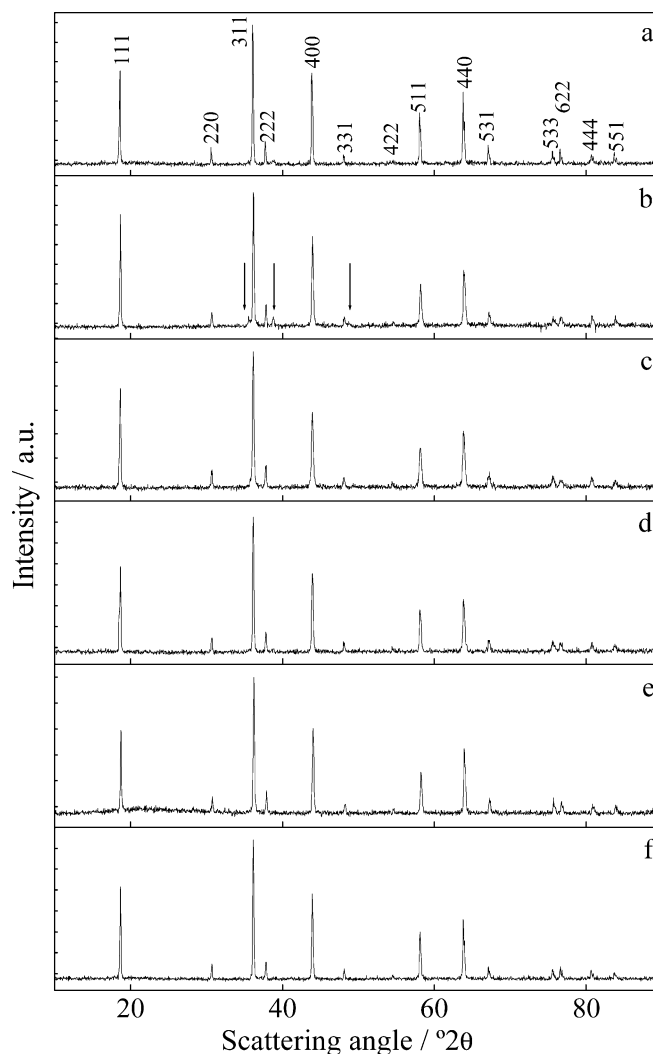


Fig. 1 Experimental X-ray diffraction spectra of samples $\text{LiCu}_x\text{Mn}_{2-x}\text{O}_4$, where $x=0.5$ (a), 0.55 (b) and 0.45 (c) and of $\text{LiCu}_{0.49}\text{Al}_{0.01}\text{Mn}_{1.5}\text{O}_4$ (d), $\text{LiCu}_{0.45}\text{Al}_{0.05}\text{Mn}_{1.5}\text{O}_4$ (e) and $\text{LiCu}_{0.45}\text{Ti}_{0.05}\text{Mn}_{1.5}\text{O}_4$ (f)

oxides (indicated with an arrow), which did not disappear after further thermal treatment. In contrast a high-purity spinel phase was obtained for $x=0.45$ and 0.50 in the nominal composition $\text{LiCu}_x\text{Mn}_{2-x}\text{O}_4$ (Fig. 1, patterns a and c, respectively) and for the Al-doped sample (Fig. 1, pattern d). When excess Li was used, minor impurities of Li_2MnO_3 were detected in all cases. Concerning the doped phases, a pure material was obtained except in the case of boron. The 220 diffraction line was clearly visible in the patterns of all the samples synthesized (Fig. 1). The intensity of this Bragg reflection could be indicative of a significant amount of copper residing on the tetrahedral sites of the spinel structure. Taking this into account, a detailed chemical analysis of the products was carried out by atomic absorption spectroscopy of some selected samples. The data for the samples with nominal composition $\text{LiCu}_{0.5}\text{Mn}_{1.5}\text{O}_4$ (stoichiometric and lithium-excess synthesis) and $\text{LiCu}_{0.49}\text{Al}_{0.01}\text{Mn}_{1.5}\text{O}_4$ (stoichiometric synthesis) showed

Table 1 Nominal composition and sample composition obtained from atomic absorption and Rietveld analysis. *M* is the gram equivalent of Cu plus Mn per 100 g of sample

Nominal		Atomic absorption		Rietveld analysis		Titration
Composition	<i>M</i>	Sample composition	<i>M</i>	Spinel composition	<i>M</i>	<i>M</i>
LiCu _{0.5} Mn _{1.5} O ₄	1.08	Li _{0.72} Cu _{0.60} Mn _{1.73} O ₄	1.15	Li _{0.64} Cu _{0.61} Mn _{1.75} O ₄	1.16	1.14
LiCu _{0.5} Mn _{1.5} O ₄ ^a	1.08	Li _{0.70} Cu _{0.54} Mn _{1.59} O ₄	1.12	Li _{0.70} Cu _{0.54} Mn _{1.59} O ₄	1.12	1.12
LiCu _{0.49} Al _{0.01} Mn _{1.5} O ₄	1.08	Li _{0.70} Cu _{0.61} Al _{0.01} Mn _{1.74} O ₄	1.15	Li _{0.64} Cu _{0.60} Al _{0.01} Mn _{1.75} O ₄	1.16	1.14
LiCu _{0.45} Al _{0.05} Mn _{1.5} O ₄	1.08	Li _{0.69} Cu _{0.52} Al _{0.05} Mn _{1.70} O ₄	1.13	Li _{0.70} Cu _{0.52} Al _{0.05} Mn _{1.73} O ₄	1.13	1.12

^aSample prepared with 5% lithium excess during synthesis

that only about 0.70 Li was incorporated in the spinel structure (Table 1). The low amount of Li incorporated in the spinel phase is noticeable, even in samples prepared with lithium excess. This fact is ascribable to the location of copper in tetrahedral sites preventing lithium incorporation. In order to gain information about the cation distribution in these spinels, selected refinement analyses were carried out by the Rietveld method. These results are shown in Table 2 for the three selected spinel phases and agree well with the chemical composition obtained by atomic absorption. Furthermore, the amount of copper on the tetrahedral sites could be estimated to 0.36, 0.29 and 0.36 for LiCu_{0.5}Mn_{1.5}O₄ (stoichiometric and lithium-excess synthesis) and LiCu_{0.49}Al_{0.01}Mn_{1.5}O₄ (stoichiometric synthesis), respectively. Thus, the cation distribution in these samples can be expressed in spinel notation as (Li_{0.64}Cu_{0.36})_{8a}[Cu_{0.25}Mn_{1.75}]_{16d}O₄, (Li_{0.70}Cu_{0.29})_{8a}[Cu_{0.25}Mn_{1.59}]_{16d}O₄ and (Li_{0.64}Cu_{0.36})_{8a}[Cu_{0.24}Al_{0.01}Mn_{1.75}]_{16d}O₄, respectively.

X-ray absorption at the Mn L₂₃ edge

Some selected samples were investigated by X-ray absorption spectroscopy. The X-ray absorption spectra at the Mn L₂₃ edge of MnO₂, LiCu_{0.5}Mn_{1.5}O₄ and LiCu_{0.49}Al_{0.01}Mn_{1.5}O₄ samples (Table 3) are shown in

Fig. 2. The spectra correspond to Mn(2*p*) → Mn(3*d*) transitions, split into an L₃ and an L₂ absorption edge by the spin-orbit interaction in the Mn(2*p*) ground state. The electronic configurations of Mn³⁺ and Mn⁴⁺ are 3*d*⁴ and 3*d*³, respectively. These *d* electrons are strongly localized in rather atomic-like orbitals. The Coulomb interaction between all 3*d* electrons (3*d*–3*d*) and between the 3*d* electrons and the 2*p* core hole (3*d*–2*p*) together with the 2*p* and 3*d* spin-orbit coupling leads to a multiplet of accessible states. The complex shape especially of the L₃ edge reflects the number of allowed transitions. The line shape depends critically on the local symmetry and the electronic configuration [10, 11] and can therefore be used as a diagnostic tool for changes in the lattice site or the oxidation state. In contrast to L₃, the L₂ edge is rather unstructured, but its position varies strongly with the Mn oxidation number and allows the mean oxidation number to be determined [12]. A simple visual inspection of the Mn L₃ edge shows that the profiles of sample LiCu_{0.5}Mn_{1.5}O₄ (lithium-excess synthesis) are very similar to the profile of MnO₂, and thus an oxidation state close to 4+ can be assumed for Mn in these compounds. The structures labelled I and III at the Mn L₃ edge characterize the Mn⁴⁺ oxidation state, as found in MnO₂, while the peak labelled C is observed in Mn₂O₃ [13], and characterizes Mn³⁺. This peak is weak in sample LiCu_{0.5}Mn_{1.5}O₄ (lithium-excess synthesis), but

Table 2 Summary of crystallographic data and structure refinement of the LiCu_{0.5-y}M_yMn_{1.5}O₄ solid solution

	Nominal Composition		
	LiCu _{0.5} Mn _{1.5} O ₄	LiCu _{0.5} Mn _{1.5} O ₄ ^a	LiCu _{0.49} Al _{0.01} Mn _{1.5} O ₄
Crystal system	Cubic		
Space group	<i>Fd</i> $\bar{3}m$ (227)		
<i>Z</i>	8		
<i>a</i> /Å	8.2398 (2)	8.2348 (3)	8.2382 (4)
<i>x</i>	0.2589 (6)	0.2617 (6)	0.2623 (6)
Reliability factors			
<i>R</i> _{wp}	0.0986	0.0991	0.103
<i>R</i> _{expected}	0.0834	0.0821	0.0897
GoF	1.18	1.12	1.14
<i>R</i> _{Bragg}	0.0547	0.0328	0.0515
<i>R</i> _F	0.0392	0.0279	0.0383
Occupancy			
Li	5.2 (1)	5.60 (8)	5.16 (8)
[Cu] 8a	2.8 (1)	2.28 (8)	2.84 (8)
[Cu] 16d	2.0 (1)	2.03 (8)	1.94 (8)
[Mn] 16d	14.0 (1)	12.72 (8)	13.98 (8)
[O] 32e	32	32	32

^aSamples prepared with 5% lithium excess during synthesis

Table 3 Nominal composition of samples studied by X-ray absorption, indicating their nominal composition and Mn oxidation number calculated from the effective composition and determined experimentally from the L_2 line position

Nominal composition	Mn formal oxidation state		
	Atomic absorption	Rietveld	X-ray absorption
$\text{LiCu}_{0.5}\text{Mn}_{1.5}\text{O}_4$	+ 3.50	+ 3.51	+ 3.30
$\text{LiCu}_{0.5}\text{Mn}_{1.5}\text{O}_4^a$	+ 3.91	+ 3.91	+ 3.90
$\text{LiCu}_{0.49}\text{Al}_{0.01}\text{Mn}_{1.5}\text{O}_4$	+ 3.49	+ 3.50	+ 3.30
$\text{LiCu}_{0.45}\text{Al}_{0.05}\text{Mn}_{1.5}\text{O}_4$	+ 3.60	+ 3.53	–

^aSamples prepared with 5% lithium excess during synthesis

is clearly present in samples $\text{LiCu}_{0.5}\text{Mn}_{1.5}\text{O}_4$ and $\text{LiCu}_{0.49}\text{Al}_{0.01}\text{Mn}_{1.5}\text{O}_4$ (both stoichiometric synthesis).

The relative position of the Mn L_2 edge, taken at its maximum, as a function of the Mn oxidation state, based on the spectra of the reference compounds Mn, MnO, MnO_2 , and KMnO_4 , is shown in Fig. 3. A straight line is obtained from Mn to MnO_2 ; permanganate deviates from this line, which is probably due to the lower Mn coordination number of 4 instead of 6 in the oxides. From this curve, we determine the mean Mn oxidation numbers of our samples as +3.9 for $\text{LiCu}_{0.5}\text{Mn}_{1.5}\text{O}_4$ (lithium-excess synthesis) and +3.3 for $\text{LiCu}_{0.5}\text{Mn}_{1.5}\text{O}_4$ and $\text{LiCu}_{0.49}\text{Al}_{0.01}\text{Mn}_{1.5}\text{O}_4$ (both stoichiometric syntheses). The values are in good agreement with the oxidation states calculated on the basis of the effective stoichiometry determined by atomic absorption spectroscopy, assuming formal oxidation states of +1 for Li and +2 for Cu (Table 3). The good agreement confirms the assumption of copper being predominantly

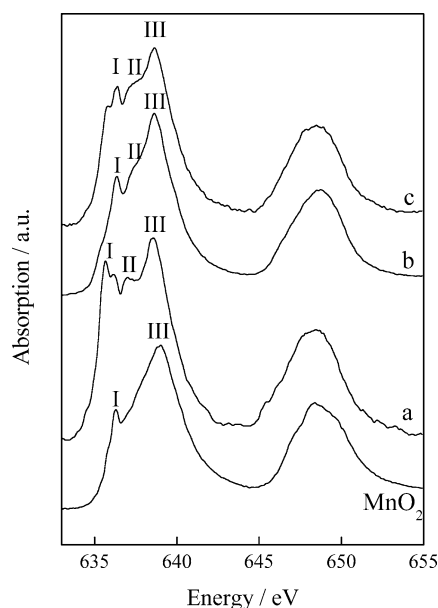


Fig. 2 Mn L_{23} edge absorption spectra of MnO_2 and samples $\text{LiCu}_{0.5}\text{Mn}_{1.5}\text{O}_4$ (a), $\text{LiCu}_{0.5}\text{Mn}_{1.5}\text{O}_4$ (lithium excess during synthesis) (b) and $\text{LiCu}_{0.49}\text{Al}_{0.01}\text{Mn}_{1.5}\text{O}_4$ (c)

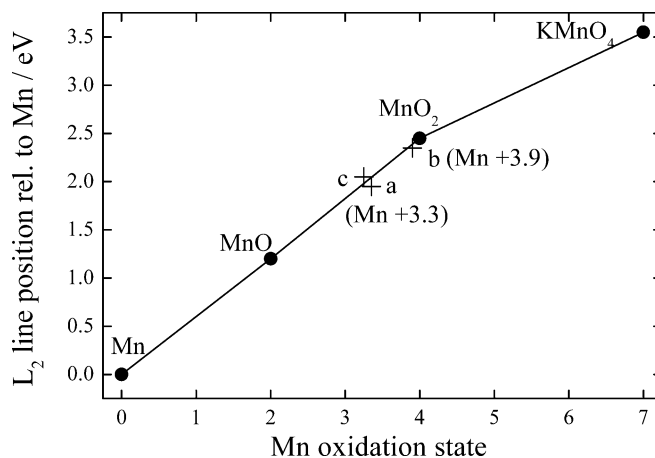


Fig. 3 Determination of the Mn oxidation number from the Mn L_2 line position relative to Mn metal: $\text{LiCu}_{0.5}\text{Mn}_{1.5}\text{O}_4$ (a), $\text{LiCu}_{0.5}\text{Mn}_{1.5}\text{O}_4$ (lithium excess during synthesis) (b) and $\text{LiCu}_{0.49}\text{Al}_{0.01}\text{Mn}_{1.5}\text{O}_4$ (c)

in the +2 valence state. The results justify the use of lithium excess during the synthesis as a key factor to control the formal oxidation state of the final product.

Electrochemical study

Electrochemical studies were carried out to compare the effect on the performance of the different synthesis conditions (stoichiometric versus lithium-excess synthesis) and the sample composition (Al, B, Co, Fe and Ti doping in $\text{LiCu}_{0.5-y}\text{M}_y\text{Mn}_{1.5}\text{O}_4$, where $y=0.01$ and 0.05 for the Al-doped sample and $y=0.05$ for the other doped compositions). The cyclic voltammetry curves of lithium-anode cells using selected spinel samples as the active cathode material are shown in Fig. 4. The scans were recorded in a potential range between 3.1 and 5.1 V versus the Li/Li^+ pair. For all samples a double intensity peak is visible at about 4.25 and 4.35 V during cell charge and at about 3.8 and 4.1 V during discharge, which is also usually found in well-crystallized LiMn_2O_4 . The integration of the curves in Fig. 4 was used to obtain the amount of lithium extracted during charge and inserted during discharge in the spinel structure, which never surpassed 0.7 Li. These results are similar to those previously reported [14].

Finally, the changes in capacity for the first few cycles for each composition are compared in Fig. 5. Concerning the undoped material, $\text{LiCu}_{0.5}\text{Mn}_{1.5}\text{O}_4$, the reversible capacity values obtained in this study were close to 90 mAh/g. As previously shown, the use of lithium excess during the synthesis results in an increase of the Mn formal oxidation state, being closer to 4+ than in samples synthesized with stoichiometric amounts of lithium. Thus, the reversible capacities in the 4-V region should decrease. In fact, the electrochemical tests of the $\text{LiCu}_{0.5}\text{Mn}_{1.5}\text{O}_4$ sample obtained using lithium excess showed a net decrease of about 15 mAh/g in the total reversible capacity (Fig. 5). Concerning the doped

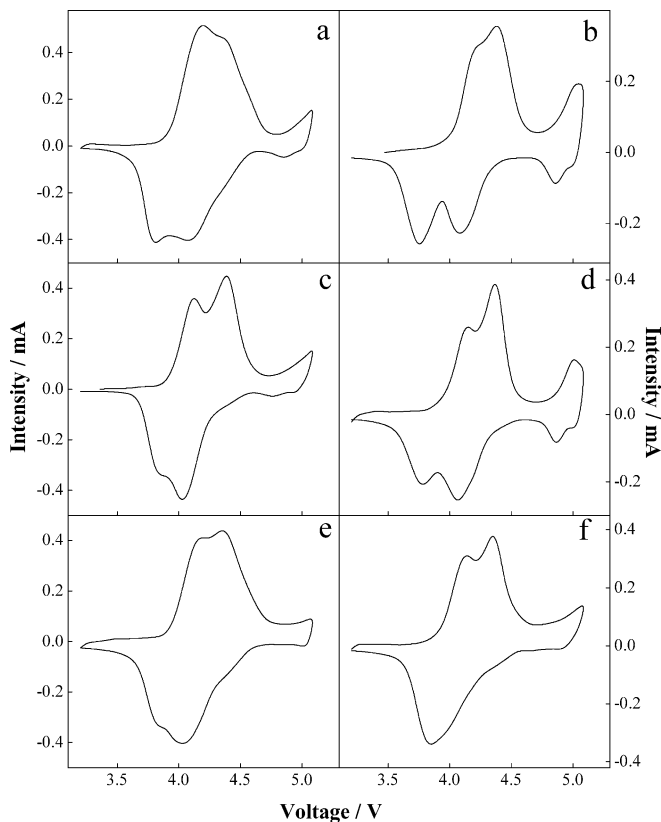


Fig. 4 Cyclic voltammograms of $\text{LiCu}_{0.5-y}\text{M}_y\text{Mn}_{1.5}\text{O}_4$: $y=0$ (a), $y=0$ and lithium-excess synthesis (b), $M=\text{Al}$, $y=0.01$ (c), $M=\text{Al}$, $y=0.01$ and lithium-excess synthesis (d), $M=\text{Al}$, $y=0.05$ (e), and $M=\text{Ti}$, $y=0.05$ (f) spinels in 1 M LiPF_6 in 1:1 wt % ethylene carbonate/diethyl carbonate electrolyte. Scan rate 50 mV/0.1 h

materials, it is worth noting that Al doping has a positive effect on capacity, as a result of maintaining low average oxidation states of manganese (Table 3); however, the special increase in capacity observed for 0.05 Al per formula in Fig. 5 implies additional effects than the decrease in oxidation state. A structural stabilization effect for an Al content above 0.01 can be suggested to explain the high capacity and good retention during the first cycles.

Conclusions

The chemical composition and cation distribution of selected members of the $\text{LiCu}_x\text{Mn}_{2-x}\text{O}_4$ series and the $\text{LiCu}_{0.5-y}\text{M}_y\text{Mn}_{1.5}\text{O}_4$ doped materials has been determined for $(\text{Li}_{0.64}\text{Cu}_{0.36})_{8a}[\text{Cu}_{0.25}\text{Mn}_{1.75}]_{16d}\text{O}_4$, $(\text{Li}_{0.70}\text{Cu}_{0.29})_{8a}[\text{Cu}_{0.25}\text{Mn}_{1.59}]_{16d}\text{O}_4$ and $(\text{Li}_{0.64}\text{Cu}_{0.36})_{8a}[\text{Cu}_{0.24}\text{Al}_{0.01}\text{Mn}_{1.75}]_{16d}\text{O}_4$. The oxidation states of manganese and copper, as determined from X-ray absorption spectroscopy evidence the following: (1) manganese is reduced below 4+ in all these solids; (2) a lithium-excess synthesis leads to a considerably higher average oxidation state of manganese and (3) copper is predominantly present as Cu(II). Finally the electrochemical results

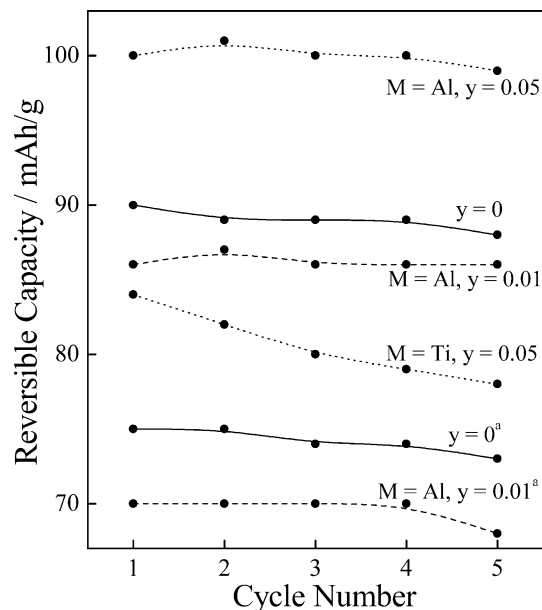


Fig. 5 Cell capacity versus cycle number for the first five cycles of lithium cells using $\text{LiCu}_x\text{Mn}_{2-x}\text{O}_4$ and $\text{LiCu}_{0.5-y}\text{M}_y\text{Mn}_{1.5}\text{O}_4$ obtained by using stoichiometric and lithium-excess synthesis (superscript a)

evidence the lack of improvement in capacity by using lithium-excess synthesis, while a significant increase in capacity is obtained by Al doping.

Acknowledgements The authors acknowledge financial support from the European Commission (contract ENK6-CT2000-00082, Negelia) and CICYT (contracts MAT2002-00434 and MAT2000-2721-CE). The authors are grateful to P. Parent and C. Laffon of the LURE staff for their assistance in recording X-ray spectra.

References

1. Wakihara M (2001) Mater Sci Eng R 33:109
2. Winter M, Besenhard JO, Spahr ME, Novak P (1998) Adv Mater 10:725
3. Ohzuku T, Ariyoshi K, Takeda S, Sakai Y (2001) Electrochim Acta 46:2327
4. Bonino F, Panero S, Satolli D, Scrosati B (2001) J Power Sources 97–98:389
5. Ein-Eli Y, Vaughney J, Thackeray MM, Mukerjee S, Yang XQ, McBreen J (1999) J Electrochem Soc 146:908
6. Hwang BJ, Santhanam R, Hu SG (2002) J Power Sources 108:250
7. Hong KJ, Sun YK (2002) J Power Sources 109:427
8. Ein-Eli Y, Howard WF (1997) J Electrochem Soc 144:L205
9. Alcántara R, Lavela P, Tirado JL, Zhecheva E, Stoyanova R (1999) J Solid State Electrochem 3:121
10. van der Laan G, Kirkman IW (1992) J Phys Condens Matter 4:4189
11. Zaanen J, Sawatzky GA, Fink J, Speier W, Fuggle JC (1985) Phys Rev B 32:4905
12. Paterson JH, Krivanek OL (1990) Ultramicroscopy 32:319
13. Liu RS, Jang LY, Chen JM, Tsai YC, Hwang YD, Liu RG (1997) J Solid State Chem 128:326
14. Ein-Eli Y, Howard WF, Lu SH, Mukerjee S, McBreen J, Vaughney JT, Thackeray MM (1998) J Electrochem Soc 145:1238